Rheological Properties and Conformation of a Side-Chain Liquid Crystal Polysiloxane Dissolved in a Nematic Solvent

Yiqiang Zhao,[†] Shaosheng Dong,[†] Alex. M. Jamieson,*[,†] Xuesong Hu,[‡] Jyotsana Lal,[‡] Sergei Nazarenko,[§] and Stuart J. Rowan[†]

Department of Macromolecular Science & Engineering, Case Western Reserve University, Cleveland, Ohio 44106-7202; Intense Pulsed Neutron Source, Argonne National Laboratory, Argonne, Illinois 60439; and School of Polymers and High Performance Materials, The University of Southern Mississippi, Hattiesburg, Mississippi 39406

Received March 7, 2005

ABSTRACT: We report measurements of the change in electrorheological response of the low molar mass nematic pentylcyanobiphenyl (5CB) on dissolution of small amounts of a side-chain liquid crystal polymer (SCLCP). From the ratio of the intrinsic viscosities with the field on and off, $[\eta_{on}]$ and $[\eta_{off}]$, respectively, we deduce a value for the ratio of the rms end-to-end distances of the SCLCP parallel and perpendicular to the nematic director, $R_{||}/R_{\perp} = 1.17 \pm 0.02$ via application of the Brochard hydrodynamic model, which indicates that the polymer has a slightly prolate shape. Small-angle neutron scattering measurements reveal a numerically similar value for the corresponding ratio of apparent rms radii of gyration, $R_{g||}/R_{g\perp} = 1.12 \pm 0.06$, for the SCLCP dissolved in deuterated 5CB. Observations of the shear stress transient response of a homeotropic monodomain indicate that, at a concentration between 0.01 and 0.02 g/mL, the solution exhibits a transition from director-aligning to director-tumbling behavior. This result is inconsistent with the Brochard model, which predicts such a transition only for a polymer with an oblate shape but agrees with a modified version, which assumes an additional contribution to viscous stress arises due to elastic coupling between the solvent and polymer directors.

Introduction

Composite materials consisting of polymers and low molar mass nematics (LMMN) are of current interest for application in electrooptic devices. The switching rates of such devices are potentially influenced by the fact that dissolved polymer causes an increase in viscosity whose origin is similar to that which occurs in solutions of polymers in isotropic solvents.[1,2] However, since nematic solutions are anisotropic, the viscometric behavior is more complex since a variety of distinct viscosity coefficients can be measured. A theoretical analysis by Brochard[1] predicts that, depending on its chain conformation (specifically a prolate vs oblate shape), the dissolved polymer may influence these viscosities differently. Several groups have investigated experimentally the viscometric properties of dilute solutions of an LCP in a nematic solvent and qualitatively confirmed various predictions of the Brochard theory.[2−16] For example, the model predicts[1] increments in the Miesowicz viscosities ($\delta\eta_b$ and $\delta\eta_c$) due to the dissolution of LCPs, which have been tested by analysis of the change in electrorheological (ER) response, identifying the field-on viscosity $\eta_{on} = \eta_c$ and field-off viscosity $\eta_{off} \approx \eta_b$ (strictly valid only for flow-aligning nematics). A strong dependence was observed with respect to LCP architecture.[22,23] Specifically, the magnitude of ER response, $\Delta\eta = \eta_{on} - \eta_{off}$, decreases in the order main-chain ≫ side-on side-chain > end-on side-chain LCP.[22,23] These results are intuitively consistent with the Brochard theory, provided the conformation of the main-chain LCP is highly prolate ($R_{||} \gg R_{\perp}$), the side-on side-chain LCP is moderately prolate ($R_{||} > R_{\perp}$), and the end-on side-chain LCP is quasi-spherical ($R_{||} \approx R_{\perp}$, $\delta\eta_{on} \approx \delta\eta_{off}$). Such conformational differences are indeed to be expected on the basis of chain statistical theory[26,27] as well as experimental observation via small-angle X-ray scattering (SAXS)[17,18] and small-angle neutron scattering (SANS).[19,20] It was further found that the molecular weight and temperature dependence of $\delta\eta_{on}$ and $\delta\eta_{off}$ could be interpreted quantitatively via the Brochard theory for both main-chain[22−24] and side-chain[22,23,25,28] LCPs, in terms of the molecular weight and temperature dependence of $R_{||}/R_{\perp}$ and the chain conformational relaxation time (τ_r).

Of additional interest is the fact that the hydrodynamic theory of Brochard predicts that dissolution of a sufficient quantity of an oblate ($R_{\perp} > R_{||}$) side-chain LCP in a flow-aligning nematogen ($\alpha_2 \ll 0$, $\alpha_3 < 0$) will produce a transition to tumbling flow ($\alpha_2 < 0$, $\alpha_3 > 0$, $-1 < \lambda < 1$)[13] and that a flow-tumbling nematogen ($\alpha_2 < 0$, $\alpha_3 > 0$) can be converted to flow-aligning behavior by dissolution of a sufficient amount of a prolate ($R_{||} > R_{\perp}$) main-chain LCP ($\delta\alpha_3 < 0$, $\lambda > 1$).[14] Experimentally, from observations of the shear stress transient of a homeotropic nematic monodomain, we have demonstrated that dissolution of a side-chain LCP in the flow-aligning nematic pentylcyanobiphenyl (5CB) produces tumbling flow[13] and that a solution of a main-chain LCP, in flow-tumbling octylcyanobiphenyl (8CB), exhibits flow-aligning behavior.[14] These results may be viewed as in qualitative agreement with the Brochard model; however, no independent verification of the LCP conformation was obtained for either system. A further prediction, for an oblate LCP dissolved in a flow-aligning nematic, that dissolution of additional LCP will cause a second transition from tumbling flow to flow aligning with the director oriented along the shear gradient ($\alpha_2 > 0$ and $\alpha_3 > 0$, $\lambda < -1$) was recently confirmed

[†] Case Western Reserve University.
[‡] Argonne National Laboratory.
[§] The University of Southern Mississippi.
* Corresponding author: Fax +1-216-3684202; e-mail alexander.jamieson@case.edu.

10.1021/ma050485h CCC: $30.25
Published on Web 05/20/2005

experimentally by Kornfield et al.[21] Moreover, preliminary small-angle neutron scattering (SANS) studies confirm an oblate conformation for this side-chain LCP.[21]

While the above rheological behavior of dilute nematic solutions of LCPs appears to agree with the Brochard model, on more detailed analysis of our data, we found certain discrepancies. First, when dissolution of a side-chain LCP in a flow-aligning LMMN causes an aligning to tumbling transition, the increments in Leslie viscosities derived from analysis of stress transient data indicate $\delta\alpha_3 > 0$ but $\delta\alpha_2 < 0$,[13−15] in contradiction to the theory which predicts

$$\delta\alpha_2 = \frac{R_\perp^2 - R_\parallel^2}{R_\perp^2}\left(\frac{ckT}{N}\right)\tau_r \quad (1)$$

$$\delta\alpha_3 = \frac{R_\perp^2 - R_\parallel^2}{R_\parallel^2}\left(\frac{ckT}{N}\right)\tau_r \quad (2)$$

where $R_\parallel$ and $R_\perp$ are the rms end-to-end distances of the LCP measured parallel and perpendicular to the director, respectively, c is the LCP concentration, k is Boltzmann's constant, T is the absolute temperature, $N = M/N_A$ is the molecular mass of the LCP, and τ_r is the conformational relaxation time of the chain. Equations 1 and 2 require that $\delta\alpha_2$ and $\delta\alpha_3$ must always have the same sign. Second, values of $R_\parallel/R_\perp$, deduced from ER data using the Brochard model, were observed to be in disagreement with those deduced from stress transient results, using the Brochard predictions for the Leslie viscosities (eqs 1 and 2). This was most apparent for LCPs with relatively small anisotropies. For example,[15] we found that LCPs, which were slightly prolate ($R_\parallel > R_\perp$) based on ER data, produce a tumbling transition, when dissolved in a flow-aligning solvent (i.e., $\delta\alpha_3 > 0$). However, as noted above, theory (cf. eqs 1 and 2) predicts such a transition can happen only if the LCP has an oblate anisotropy ($R_\parallel < R_\perp$). A third discrepancy was encountered when values of the increment in twist viscosity, measured by electric-field-dependent dynamic light scattering (EFDLS) for an SCLCP having $R_\parallel/R_\perp \sim 1$, were found to be substantially larger than predicted by the theory (viz. $\delta\gamma_1 \sim 0$).[30,31]

To rationalize these discrepancies, a phenomenological modification of the Brochard hydrodynamic model was proposed by Yao and Jamieson[15] which results in improved agreement with experiment. In particular, the theory enables a self-consistent treatment of ER data, stress transient data, and EFDLS results on solutions of a polysiloxane side-chain LCP in various LMMNs.[15,29−31] The modification is based on the assumption that for a LCP/LMMN solution an additional contribution to the hydrodynamic torque can arise from an elastic coupling between the LMMN director and the LCP director.[15]

In the present work, we provide a further test of the hydrodynamic theory, using SANS measurements to directly probe the anisotropic radii of gyration $R_{g\parallel}$ and $R_{g\perp}$ of a side-chain polysiloxane LCP with cyanobiphenyl mesogenic side group dissolved in deuterated 4′-pentyl-4-cyanobiphenyl (5CB). The value of the conformational anisotropy, as characterized by the ratio $R_{g\parallel}/R_{g\perp}$, is compared with $R_\parallel/R_\perp$ values deduced from rheological data (ER and stress transient).

Scheme 1. Chemical Structures and Phase Transition Temperatures of the Side-Chain Polysiloxane LCP (SCLCP) and the Nematic Solvent 5CB

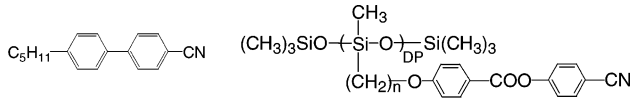

5CB (k22.8 °C n35.1 °C iso)

Side-chain polysiloxane LCP (n=5)

T_g16 °C k42 °C S_m149 °C iso

Table 1. Molecular Weights of Side-Chain Liquid Crystal Polysiloxane (n = 5)

GPC$_{PSt}$[a]			true MW[b]		
M_w (×10^3 g/mol)	M_n (×10^3 g/mol)	PDI	DP$_n$[c]	$M_{w,true}$ (×10^3 g/mol)	$M_{n,true}$ (×10^3 g/mol)
24.1	12.7	1.90	71	49.8	26.2

[a] Apparent molecular weight measured by GPC in THF as solvent at 25 °C, relative to polystyrene standards. [b] True molecular weights calculated from DP$_n$ and GPC PDI. [c] DP$_n$ = true number-average degree of polymerization of backbones based on ^{1}H NMR analysis.

Scheme 2. Deuterium Content and Phase Transition Temperatures of the d-5CB Sample

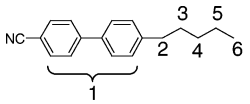

Deuteration percentage:
1: 93%; 2: 87%; 3: 72%;
4,5: 76%; 6: 87%.

d-5CB (k19.8 °C n36.8 °C iso)

Experimental Section

Materials and Sample Preparation. The chemical structures of the side-chain liquid crystal polysiloxane (SCLCP) with spacer length n = 5 and degree of polymerization (DP = 71) and nematic solvent 4′-pentyl-4-cyanobiphenyl (5CB) are given in Scheme 1, both with cyanobiphenyl LC mesogenic group. Details of the synthesis and characterization of SCLCPs are given elsewhere.[32] 5CB was purchased from Aldrich and used as received. l-α-Lecithin was purchased from Sigma Chemical Co. and used as a 0.35 wt % solution in ethanol. The molecular weights measured by GPC (Varian GPC) in THF as solvent, relative to polystyrene standards, as well as the true number-average DP determined by ^{1}H NMR (Varian Gemini NMR 200 MHz spectrometer) are listed in Table 1.

To prepare the dilute nematic solutions, a specified weight of SCLCP was dissolved in 5CB at a temperature (∼60 °C) well above its clearing point. Equilibration was continued (typically for 24 h) until complete dissolution to form an isotropic solution. A miscible nematic solution (0.02 g/mL) was observed by polarized optical microscopy (POM), using an Olympus optical polarizing microscope equipped with a Mettler FP82 hot stage and a Mettler FP800 central processor to check its homogeneity, and further confirmed by DSC measurement showing a slightly increased T_{ni} = 35.6 °C with a biphasic region of 1.7 °C. The overlap concentration c^* of the SCLCPs in 5CB was estimated using $c^* \approx 2.5/[\eta_{off}]$, where $[\eta_{off}]$ is obtained from ER measurement with the field off. This gives c^* in a range of 0.10−0.22 g/mL for the SCLCP solutions at the tested temperatures (23−40 °C), and therefore our experiments were conducted at concentrations less than ∼0.08 g/mL.

Deuterated 5CB (d-5CB) was synthesized for use as a nematic solvent in the SANS experiments. The synthesis route is a modified version[32] of that described elsewhere.[33] The d-5CB has deuterium ratios estimated from ^{1}H NMR analysis and phase transition temperatures as shown in Scheme 2. The nematic range of our d-5CB is consistent with reported results.[33] POM images indicate the d-5CB exhibits a typical threaded texture in the nematic state.

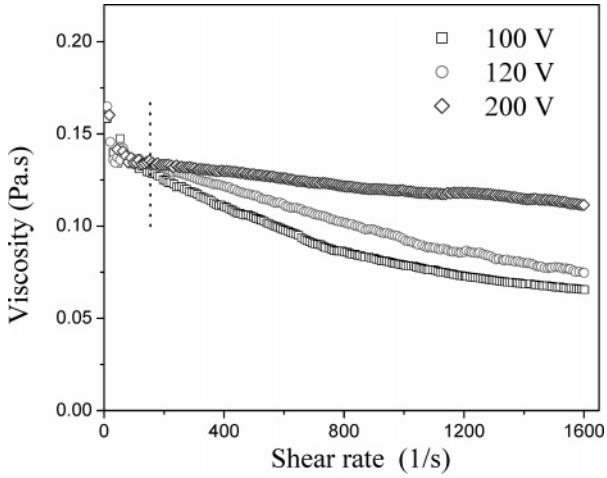

Figure 1. Shear rate dependence of the apparent viscosity at different applied voltages for 0.04 g/mL side-chain LCP (n = 5, DP = 37) in 5CB at 23 °C.

Rheological Measurements. ER shear sweep experiments were performed on a Carri-Med controlled-stress rheometer using cone-and-plate geometry (cone angle = 0.5°, cone radius = 1 cm). A voltage of 100 V was applied to the cone via a mercury bath by a Bertan model 215 high-voltage power supply. With a gap of 15 μm, the resulting electric field is E = 2.2 kV/mm, computed as the mean value integrated from the cone tip to the rim. As shown in earlier work[22−25] and illustrated in Figure 1, this field is high enough to ensure complete alignment in the low-shear limit. Nematic samples were placed in the gap and preequilibrated at a selected temperature for at least 10 min. Under these conditions, for nematic LCP solutions of high viscosity, η_c can be obtained by extrapolation to zero shear.[22−25] The sample temperature was controlled accurately to 0.1 °C.

Transient shear flow experiments were performed on a Rheometrics RFS-8500 rheometer with stainless steel cone-and-plate geometry (cone angle = 0.02 rad and cone radius = 25 mm) at constant shear rate 4 s^{-1} using previous methodology.[13−15] The inner surfaces of the cone and the plate were treated with a 0.35 wt % ethanol solution of L-α-lecithin to achieve surface anchoring for homeotropic alignment. The sample temperature was controlled accurately to 0.1 °C. Each measurement was made 15 min after the sample was loaded or subjected to a prior test.

Small-Angle Neutron Scattering. The small-angle neutron scattering measurements (SANS) were carried out on the SAD time-of-flight small-angle diffractometer at the Intense Pulsed Neutron Source facility, Argonne National Laboratory, IL. This instrument employs neutrons with a wide range of wavelengths λ (0.9−14 Å) to produce SANS data over a wide q range (0.005−0.35 $Å^{-1}$). Here q is the scattering vector, $|\mathbf{q}| = q = 4\pi \sin\theta/\lambda$; 2θ is the scattering angle. SANS experiments were performed on a dilute solution of the hydrogenated polysiloxane SCLCP (n = 5, DP = 71) in d-5CB. The neutron scattering length density (SLD) of nematic d-5CB and a single repeat unit of the SCLCP are estimated approximately to be 4.90×10^{10} cm^{-2} (based on the measured 85.6% deuteration) and 1.82×10^{10} cm^{-2}, respectively. To obtain adequate scattering contrast, and yet remain below the overlap concentration, as discussed above, a concentration of 0.0811 g/mL was used for both nematic and isotropic solutions. Samples were contained in 1 mm path length quartz cells for measurements at test temperatures. The sample temperature was controlled accurately to 0.2 °C. For dilute nematic solutions, a magnetic field of 0.81 T was applied to produce planar alignment of the sample at nematic temperatures. The scattering data and 2-D pattern were collected and processed according to standard procedures, including the subtraction of scattering from the solvent and empty cell as background contributions. Incoherent scattering from the sample is negligible.

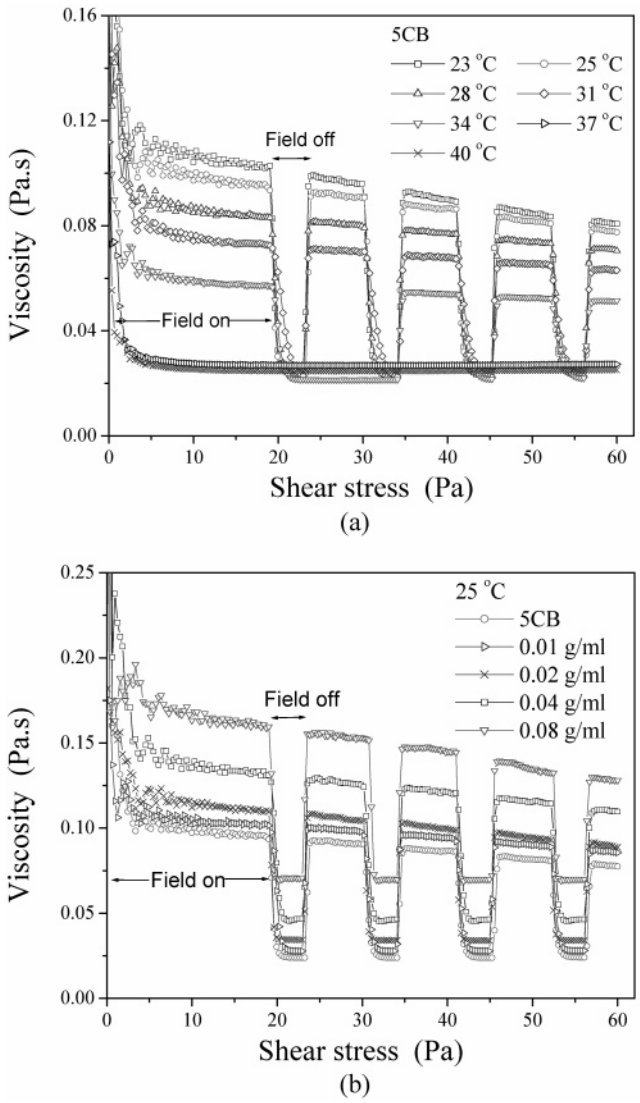

Figure 2. ER response, when the electric field is switched on and off during a controlled stress sweep, for (a) pure 5CB at different temperatures and (b) dilute solutions of a side-chain LCP (n = 5, DP = 71) in 5CB at 28 °C, for different LCP concentrations.

Results

ER Behavior of Dilute Solutions of the Side-Chain LCP in 5CB. For LCs with positive dielectric anisotropy $\Delta\epsilon$, such as 5CB, a positive ER effect is observed in the nematic range, as shown in Figure 2a. The magnitude of the increase in viscosity on application of the electric field ($\Delta\eta = \eta_{on} - \eta_{off}$) is determined by the balance between the hydrodynamic and electric torques. Thus, the apparent viscosity decreases as the stress increases until, at a sufficiently large stress, the viscous torque dominates and the director rotates toward the flow direction, generating a viscosity numerically comparable to η_{off}. The corresponding ER responses for dilute nematic solutions (0.01−0.08 g/mL) of the side-chain LCP are shown in Figure 2b, where it is seen that the field-on and field-off viscosity increase proportionally with increase of concentration. The ER magnitude $\Delta\eta$ of these solutions is similar to that of pure 5CB, implying a quasi-spherical chain conformation.[22−25] Figure 2 also demonstrates that the switching rate of the viscosity when the field is turned on or off is

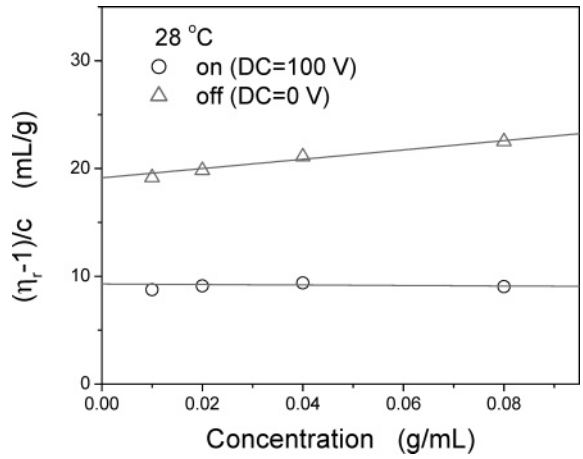

Figure 3. Huggins plots to obtain the intrinsic viscosities, $[\eta_{on}]$ and $[\eta_{off}]$, for dilute solutions of a side-chain LCP ($n = 5$, DP = 71) in 5CB at 28 °C, with the electric field respectively on and off.

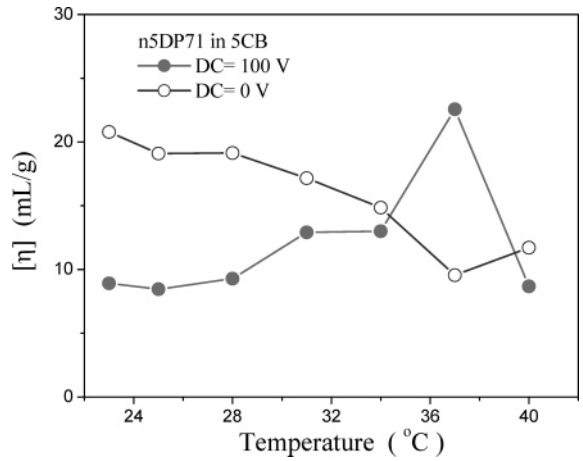

Figure 4. Temperature dependence of the intrinsic viscosities of a 5CB solution of a side-chain LCP ($n = 5$, DP = 71).

very fast for both pure 5CB and the dilute nematic solutions.[22]

Figure 3 shows Huggins plots according to the equation $(\eta_r - 1)/c = [\eta] + k_1[\eta]^2c + \ldots$ from which the intrinsic viscosities, $[\eta_{off}]$ and $[\eta_{on}]$, are extracted. The temperature dependence of $[\eta_{off}]$ and $[\eta_{on}]$ is shown in Figure 4 for solutions of the side-chain LCP in 5CB. As temperature increases, the order parameter of the nematic solvent decreases, and the interaction between the mesogens of the side-chain LCP and the nematic solvent becomes weaker. As a result, the conformation of the side-chain LCP becomes less anisotropic, and the intrinsic viscosities $[\eta_{off}]$ and $[\eta_{on}]$ become increasingly similar near the transition temperature, T_{ni}. Consistent with the microscopic observation, a biphasic transition region exists in the temperature range $T = 35-40$ °C. In the nematic state, $[\eta_{off}]$ is always larger than $[\eta_{on}]$; thus, the effective hydrodynamic volume with the field on is smaller than that with the field off. This result appears to be a common feature of end-on side-chain LCPs,[22,25,28] in contrast to main-chain LCPs and side-on SCLCPs, for which the opposite is observed, i.e., $[\eta_{off}] < [\eta_{on}]$.[22−24]

We make the assignments $[\eta_{off}] \sim [\eta_b]$ and $[\eta_{on}] = [\eta_c]$, where $[\eta_b]$ and $[\eta_c]$ are two of the Miesowicz viscosities. The approximate quantity for η_b stems from the fact that, for a flow-aligning nematic, the director aligns at a small angle to the flow direction $\theta = \tan^{-1}[(\alpha_2/\alpha_3)^{1/2}]$ and not precisely along the flow direction. We adopt expressions from the hydrodynamic model described by Brochard:[1]

$$\delta\eta_c = \left(\frac{ckT}{N}\right)\tau_r\left(\frac{R_{||}^2}{R_\perp^2}\right) \tag{3}$$

$$\delta\eta_b = \left(\frac{ckT}{N}\right)\tau_r\left(\frac{R_\perp^2}{R_{||}^2}\right) \tag{4}$$

Taking the ratio of eqs 3 and 4, we obtain a relationship between the ratio of viscosity increments and $R_{||}/R_\perp$

$$\frac{R_{||}^4}{R_\perp^4} = \frac{\delta\eta_c}{\delta\eta_b} \tag{5}$$

A quantitative interpretation of these observations is then possible via eq 5, which is strictly applicable only in the limit of infinite dilution. Thus, we utilize the reduced viscosity increments computed from the intrinsic viscosities:

$$\lim_{c\to 0} \delta\eta_c/c = \eta_c^0[\eta_c] \tag{6}$$

$$\lim_{c\to 0} \delta\eta_b/c = \eta_b^0[\eta_b] \tag{7}$$

where η_b^0 and η_c^0 are the Miesowicz viscosities of the pure solvents. We therefore compute the chain anisotropy $R_{||}/R_\perp$ from[22−25]

$$\frac{R_{||}^4}{R_\perp^4} = \frac{\eta_c^0[\eta_c]}{\eta_b^0[\eta_b]} \tag{8}$$

The magnitude of the ER response is given by[22−25,28]

$$\eta_{on} - \eta_{off} = \eta_{on}^0 - \eta_{off}^0 + c\left(\frac{\delta\eta_{on}}{c} - \frac{\delta\eta_{off}}{c}\right) = \eta_c^0 - \eta_b^0 + \left(\frac{R_{||}^2}{R_\perp^2} - \frac{R_\perp^2}{R_{||}^2}\right)\frac{ckT}{N}\tau_r \tag{9}$$

where η_{on}^0 and η_{off}^0 refer to the solvent values. From this equation, since $R_{||}R_\perp$ is known, we can now determine the molecular relaxation time τ_r. At $T = 28$ °C, $[\eta_{on}] = 9.3 \pm 0.5$ mL/g and $[\eta_{off}] = 19.1 \pm 1$ mL/g. Applying eqs 8 and 9, we find that $R_{||}/R_\perp = 1.17 \pm 0.02$, indicating a slightly prolate shape, and $\tau_r = 11.62$ μs. These results provide a molecular interpretation of the ER data.

Chain Conformation Probed by SANS. To directly estimate the chain anisotropy, we carried out SANS measurements on the hydrogenated polysiloxane SCLCP dissolved in d-5CB in the nematic (28 °C) and isotropic (40 °C) states with planar alignment under a high magnetic field (0.81 T). To obtain sufficient contrast and remain below the overlap concentration, a solution of concentration 0.0811 g/mL was used for SANS measurements. The resulting 2-D scattering patterns at 28 and 40 °C are exhibited in parts a and b of Figure 5, respectively. These images confirm that the chain conformations are quasi-spherical in each case. The scattering intensity in the directions parallel (q_x) and

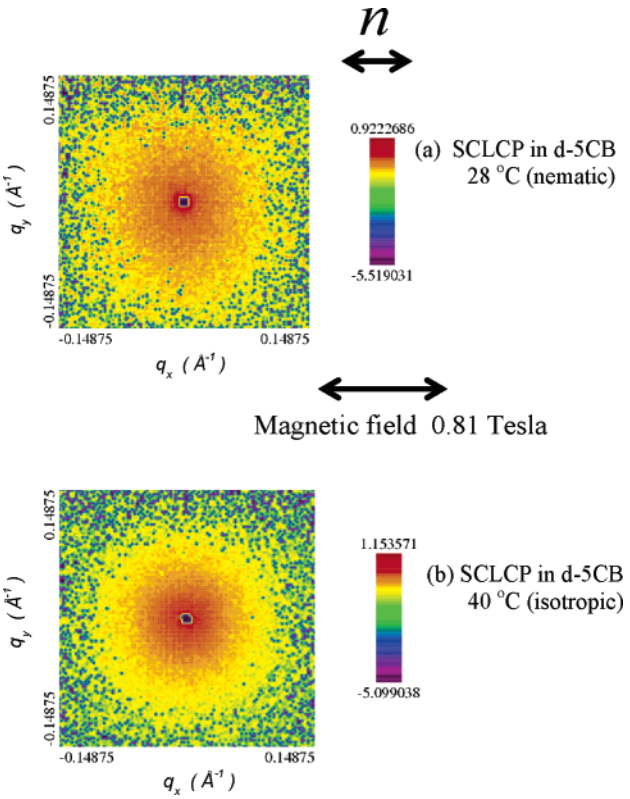

Figure 5. SANS 2-D patterns for 0.0811 g/mL side-chain LCP ($n = 5$, DP = 71) dissolved in deuterated 5CB (a) in the nematic state at 28 °C and (b) in the isotropic state at 40 °C.

perpendicular (q_y) to the nematic axis were analyzed via the Guinier approximation (eq 10) in the low q regime ($qR_g < 1$, 0.02 $Å^{-1} < q < 0.042$ $Å^{-1}$) to determine the apparent z-average mean-square radius of gyration $\langle R_g^2\rangle_z$ in the two orthogonal directions:[34]

$$I(q) = I_0 P(q) = I_0 \exp\left(-\frac{q^2\langle R_g^{\,2}\rangle_z}{3}\right) \qquad (10)$$

In the following text, for brevity, we denote $R_g = \langle R_g^2\rangle_z^{1/2}$ as the apparent rms z-average radius of gyration. Least-squares fits were performed simultaneously in both directions to ensure the same value of I_0 is used to obtain $R_{g|}$ and $R_{g\perp}$. From the Guinier fits shown in Figure 6, we determine $R_{g|} = 28 \pm 1$ Å and $R_{g\perp} = 25 \pm 1$ Å at 28 °C. Thus, the conformation is indeed found to be slightly prolate in the nematic state, viz. $R_{g|}/R_{g\perp} = 1.12 \pm 0.06$, and numerically comparable to the ratio of rms end-to-end distances deduced from ER experiments, $R_|/R_\perp = 1.17 \pm 0.02$. We point out here that, at finite concentration (0.0811 g/mL in this study), the apparent radius of gyration derived from low-q Guinier fits is influenced by polymer−solvent interactions and therefore differs from the true R_g as $R_g^{app} = R_g(I_c/I_0)^{1/2}$, where I_c is the scattering intensity at $q = 0$ at finite concentration and $I_0 = KcM$ is the "ideal" $q = 0$ intensity. It follows that nonideality corrections affect $R_{g|}$ and $R_{g\perp}$ equally, and therefore the ratio $R_{g|}/R_{g\perp}$ can justifiably be compared with the ratio $R_|/R_\perp$, deduced from ER measurements.

A complication arises, however, in that $R_|/R_\perp$ as embodied in the theory relates to the ratio of rms end-to-end distances of the LCP backbone. The relationship between $R_{g|}/R_{g\perp}$ and $R_|/R_\perp$ is nontrivial. Recently, Kempe et al.[44] carried out a study of the anisotropic

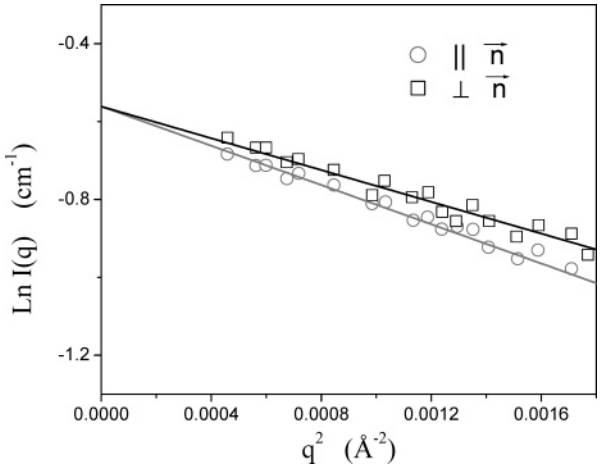

Figure 6. Guinier plot of scattered intensity from a dilute solution (0.0811 g/mL) of a side-chain LCP ($n = 5$, DP = 71) in deuterated 5CB at 28 °C.

radii of gyration of a side-chain LCP in a nematic solvent and derived expressions relating $R_{g|}$ and $R_{g\perp}$ to the corresponding radii of gyration of the polymer backbone ($R_{g|b}$ and $R_{g\perp b}$):

$$R_{g|}^{\,2} = R_{g|b}^{\,2} + \frac{L^2(2S+1)}{3} \qquad (11)$$

$$R_{g\perp}^{\,2} = R_{g\perp b}^{\,2} + \frac{L^2(1-S)}{3} \qquad (12)$$

Here L is the length of the mesogenic side group and S is the order parameter. Using the software package CS ChemBats3D Pro (CambridgeSoft Co.), we find L is ≈18 Å for our polysiloxane SCLCP. Assuming that the dilute solution has the same order parameter as the nematic solvent 5CB, i.e., $S = 0.54$ at 28 °C,[45] we utilize eqs 11 and 12 and obtain $R_{g|b} = 24 \pm 1$ Å and $R_{g\perp b} = 24 \pm 1$ Å, leading to a value for the conformational anisotropy of the backbone $R_{g|b}/R_{g\perp b} = 1.00 \pm 0.06$. This indicates the backbone conformation is spherical, within experimental error, and may be either very weakly prolate or oblate. This result is strictly inconsistent with the ER data, however, since it implies a ratio $\delta\eta_c/\delta\eta_b = 1.0 \pm 0.26$, significantly smaller than the experimental result, $\delta\eta_c/\delta\eta_b = 1.87 \pm 0.10$. Finally, we note that the application of Guinier analysis in the isotropic state leads to $R_{g|} = 38 \pm 1$ Å and $R_{g\perp} = 38 \pm 0.5$ Å at 40 °C. Hence, $R_{g|}/R_{g\perp} = 1.00 \pm 0.03$ indicating, as expected, a spherical chain conformation in the isotropic state.

Stress Transients of Dilute Solutions of the Side-Chain LCP in 5CB. 5CB exhibits transient shear flow behavior characteristic of a flow-aligning nematic with a single stress overshoot peak,[13,14] in the nematic state as shown in Figure 7. However, on dissolving a sufficient amount of the side-chain LCP (0.02 g/mL), periodic stress oscillations are clearly observed in Figure 7, indicative of a transition to director tumbling dynamic behavior. Since increased shear rates suppress the magnitude of the initial tumbling peak and result in fewer oscillation peaks, we chose to apply an optimal shear rate 4 s^{-1} for all stress transient experiments, under which conditions the strain periodicity of the tumbling behavior is obtained with good accuracy as seen in Figure 7 (Table 3). We further note parenthetically that the frequency dependence of the storage and loss moduli (G' and G''), for a 0.02 g/mL solution of the

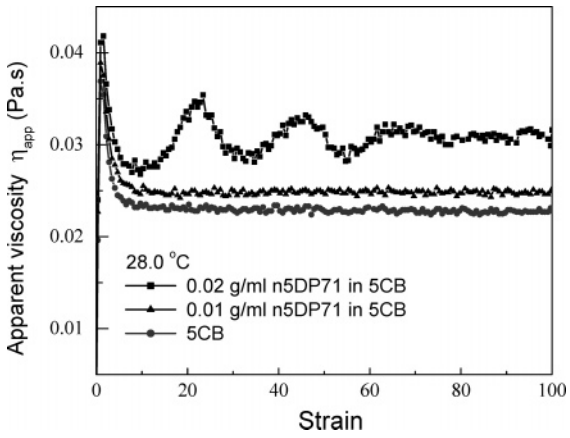

Figure 7. Transient shear flow behavior at 28.0 °C and shear rate 4 s^{-1} is shown for 0.01 and 0.02 g/mL solutions of a side-chain LCP (n = 5, DP = 71) in 5CB and compared vs pure 5CB.

Table 2. Miesowicz and Leslie Viscosities of 5CB

temp (°C)	$\eta_c \pm 0.2\%$ (Pa·s)	$\eta_b \pm 8\%$ (Pa·s)	$\alpha_2 \pm 2\%$ (Pa·s)	$\alpha_3 \pm 6\%$ (Pa·s)
23	0.1129	0.0187	−0.0878	−0.0064
25	0.1016	0.0186	−0.0775	−0.0055
28	0.0860	0.0167	−0.0645	−0.0048
31	0.0720	0.0165	−0.0516	−0.0039

Table 3. Miesowicz and Leslie Viscosities and Strain Periodicity of 0.02 g/mL Side-Chain LCP (n = 5, DP = 71) in 5CB

temp (°C)	$\eta_c \pm 1\%$ (Pa·s)	$\eta_b \pm 10\%$ (Pa·s)	$\alpha_2 \pm 3\%$ (Pa·s)	$\alpha_3 \pm 4\%$ (Pa·s)	$\gamma_p \pm 3\%$ periodicity (strain unit)
23	0.1308	0.0322	−0.1010	0.0024	20.8
25	0.1177	0.0281	−0.0916	0.0020	21.9
28	0.1017	0.0274	−0.0758	0.0015	22.5
31	0.0894	0.0242	−0.0662	0.0010	25.6

SCLCP in 5CB, indicates that we are making measurements in the terminal flow region of the solution ($G'' \gg G'$). Thus, the crossover frequency ($G' = G''$) was estimated to be ca. 794 rad/s by extrapolation of G' and G'' to high frequency, using a slope of two and one, respectively. This frequency corresponds to an approximate shear rate of 126 s^{-1}, much larger than the test shear rate of 4 s^{-1}, indicating the stress transient response is far below the frequency characteristic of the polymer chain relaxation.

Also evident in Figure 7 is the fact that the shear transient of the SCLCP solution at 0.01 g/mL shows flow-aligning behavior, indicating that the transition to tumbling flow occurs somewhere between 0.01 and 0.02 g/mL. With increase of temperature in the nematic state, the strain periodicity, γ_p, increases, and the amplitudes of the stress overshoot and oscillation peaks decrease (Table 3). At large strains, the tumbling peaks are damped due to out-of-plane motion of the director.[13,35−39] The tumbling flow signature of the solution disappears at 34 °C, and a stress overshoot at very small strain characteristic of aligning flow is present. In the isotropic state (≥35 °C), no stress overshoot is observed.

According to Ericksen's TIF theory, the transient flow behavior of a homeotropic nematic monodomain subjected to a shear flow is determined principally by two of the six Leslie coefficients, α_2 and α_3. A quantitative analysis of α_2 and α_3 is possible based on the approach developed by Gu et al.[14] and Yao et al.,[15,29] utilizing the following equations

$$\alpha_2 + \alpha_3 = \eta_b - \eta_c \tag{13}$$

$$\eta_{app} = \left[\alpha_1 + \frac{(\alpha_3 + \alpha_2)^2}{\alpha_3 - \alpha_2}\right]^2 \sin\theta^2 \cos\theta + \eta_c - \frac{\alpha_2^2}{\alpha_3 - \alpha_2} \tag{14}$$

in which η_c is obtained independently with high precision via ER measurements.[22−25] A term, $\delta\gamma$, is applied to correct for a strain delay of the stress transients resulting from mechanical inertia:

$$\tan\theta = \left(\frac{-\alpha_2}{\alpha_3}\right)^{0.5} \tan\left[\frac{(-\alpha_2\alpha_3)^{0.5}}{\alpha_3 - \alpha_2}(\gamma + \delta\gamma)\right] \quad \text{for } \alpha_3 > 0 \tag{15}$$

$$\tan\theta = \left(\frac{\alpha_2}{\alpha_3}\right)^{0.5} \tanh\left[\frac{(\alpha_2\alpha_3)^{0.5}}{\alpha_3 - \alpha_2}(\gamma + \delta\gamma)\right] \quad \text{for } \alpha_3 < 0 \tag{16}$$

To reduce the independent variables in eqs 14−16 to three, the following equation for the strain periodicity is applied:[22]

$$\gamma_p = \frac{\pi(1 + \delta^2)}{\delta} \tag{17}$$

where $\delta = (-\alpha_3/\alpha_2)^{0.5}$. Using eqs 14−17, values of α_2 and α_3 for pure 5CB and the nematic solution of the side-chain LCP in 5CB (0.02 g/mL) were determined by fitting the initial overshoot in the apparent viscosity, η_{app}. As shown Figure 8, a good fit is evident at low strains for both flow-aligning 5CB and the flow-tumbling nematic solution at 23 °C. The fitting results are tabulated in Table 2 for pure 5CB and in Table 3 for the 0.02 g/mL SCLCP solution in the nematic temperature range. The values of α_2 are negative for both the SCLCP/5CB solution and pure 5CB, whereas α_3 is negative for 5CB and positive for the solution, reflecting respectively aligning flow and tumbling flow. When temperature increases, the magnitudes of α_2 and α_3 decrease for both 5CB and the SCLCP/5CB solution. η_c values listed in Tables 2 and 3 were derived from ER measurements, and we utilized eq 13 to obtain η_b values. Use of the latter values at T = 28 °C yields a ratio of Miesowicz viscosity increments $\delta\eta_c/\delta\eta_b = 1.47 \pm 0.19$, from which insertion into eq 5 yields a value of the anisotropy ratio $R_\parallel/R_\perp = 1.10 \pm 0.05$, in numerically good agreement with the SANS measurements of the global radius ratio $R_{g\parallel}/R_{g\perp} = 1.12 \pm 0.06$ and, to a lesser extent, with the backbone radius ratio $R_{gb\parallel}/R_{gb\perp} = 1.00 \pm 0.06$.

Discussion

With regard to the ER measurement, a potential problem arises in interpreting $[\eta_{off}]$ for side-chain LCP in 5CB,[25] since the stress transient result indicates that this nematic solution at sufficiently high LCP concentration (0.02 g/mL) has positive values of the Leslie viscosity α_3 and hence exhibits flow-tumbling behavior. Under such conditions, the measured η_{off} is not well-defined because, for tumbling nematics under steady flow, the director tends to rotate out of plane toward the vorticity axis, creating defects in steady flow, as

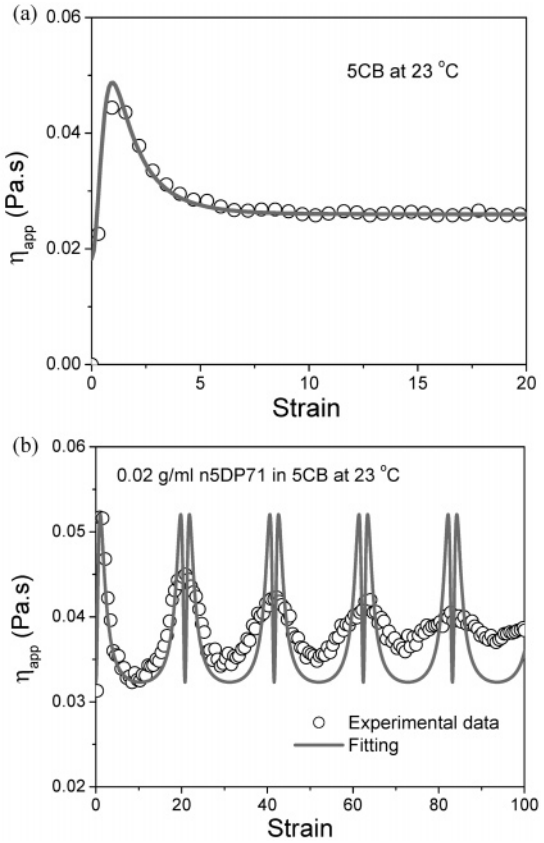

Figure 8. Theoretical fits to the stress transient data at 23 °C and shear rate 4 s^{-1}: (a) flow aligning response for pure 5CB; (b) director tumbling response for a 0.02 g/mL solution of a side-chain LCP (n = 5, DP = 71) in 5CB.

suggested from the experimental observation[40] and computer simulation.[39] Experimentally, the measured steady-shear viscosity of tumbling nematics remains small,[41] numerically comparable to the Miesowicz viscosities η_a and η_b. Here, we also note that the measured η_{off} of 0.02 g/mL SCLCP nematic solution is slightly higher by about 10−17% than the computed value η_b from eq 13, using the ER value of η_c, and α_2 and α_3 from the stress transient fits (Table 3). However, for a lower LCP concentration (0.01 g/mL), the flow-aligning character is maintained, and the measured viscosity is closer to η_b. Since determination of intrinsic viscosity involves extrapolation to zero concentration, it seems reasonable to expect that $[\eta_{off}]$ is very close to $[\eta_b]$, of the order predicted on the basis of Ericksen's TIF theory, which indicates that the flow-alignment angle is $\theta = \tan^{-1}[(\alpha_2/\alpha_3)^{1/2}]$. We also note that, in the presence of a strong electric field, theory[42] and experiment[43] confirm that the flow-tumbling phenomenon is suppressed for a nematic with positive $\Delta\epsilon$ and so we can safely make the assignment $[\eta_{on}] = [\eta_c]$. On the basis of the above, therefore, at most we may anticipate an overestimate in the ratio $R_\parallel/R_\perp$ of the order 4%. The ER result, $R_\parallel/R_\perp = 1.17 \pm 0.02$, appears to be consistent with the SANS measurements of global $R_{g\parallel}$ and $R_{g\perp}$, which yield a chain anisotropy value $R_{g\parallel}/R_{g\perp} = 1.12 \pm 0.06$ at 28 °C, but not with the backbone anisotropy, $R_{g\parallel b}/R_{g\perp b} = 1.00 \pm 0.06$.

Further problems arise when comparing the SANS measurements vs values of the Leslie and Miesowicz viscosities deduced from analysis of the stress transients. First, we note that the observation that dissolution of the side-chain LCP (n = 5, DP = 71) in flow-aligning 5CB causes a transition to tumbling flow is strictly inconsistent with the Brochard hydrodynamic model,[1] which predicts such a transition occurs only if the chain conformation is oblate ($R_\parallel/R_\perp < 1$). It is true that the backbone anisotropy deduced from the SANS data allows the possibility of a slightly oblate character, $R_{g\parallel b}/R_{g\perp b} \sim 0.94$. However, it is easy to show that the rheological data are inconsistent with this value. Thus, for the tumbling solution which has 0.02 g/mL SCLCP in 5CB at 28 °C, the prefactor $(ckT/N)\tau_r$ in eqs 3 and 4 is computed to be 0.0117 Pa·s, using $\delta\eta_c$ and $\delta\eta_b$ from the ER measurements, and 0.0129 Pa·s, using $\delta\eta_c$ from ER and $\delta\eta_b$, from eq 13 with $\delta\alpha_2$ and $\delta\alpha_3$ from stress transient data. It follows that, using the α_3 values in Tables 2 and 3, and an average value $(ckT/N)\tau_r = 0.0123 \pm 0.0005$ Pa·s from ER and stress transient results, the original Brochard model (eq 2) predicts $R_\parallel/R_\perp = 0.82 \pm 0.04$, significantly different from the SANS result, $R_{g\parallel b}/R_{g\perp b} = 1.00 \pm 0.06$. Alternatively, if we assume the chain conformation is slightly oblate with a value $R_\parallel/R_\perp \sim 0.94$, the concentration of the SCLCP estimated via the Brochard model (eq 2) to give the tumbling rheology at 28 °C is computed to be 0.08 ± 0.04 g/mL, using the stress transient data in Tables 2 and 3, much larger than experimentally observed (0.02 g/mL).

To explain these discrepancies, we previously proposed a revised model, based on the notion that reorientational motion of the SCLCP exerts an additional contribution to the torque on the solvent director because of the mechanical coupling between director and LCP mesogen orientation.[15] This leads to an additional contribution to the twist viscosity

$$\delta\gamma_1^{el} = \left(\frac{ckT}{N}\right)\tau_r \tag{18}$$

and hence a modified result for $\delta\gamma_1$ is obtained:

$$\delta\gamma_1 = \delta\alpha_3 - \delta\alpha_2 = \left[\frac{(R_\perp^2 - R_\parallel^2)^2}{R_\perp^2 R_\parallel^2} + 1\right]\left(\frac{ckT}{N}\right)\tau_r \tag{19}$$

Since $\alpha_2 = (\gamma_2 - \gamma_1)/2$ and $\alpha_3 = (\gamma_2 + \gamma_1)/2$, it follows that

$$\delta\alpha_2 = \left(\frac{1}{2} - \frac{R_\parallel^2}{R_\perp^2}\right)\left(\frac{ckT}{N}\right)\tau_r \tag{20}$$

$$\delta\alpha_3 = \left(\frac{R_\perp^2}{R_\parallel^2} - \frac{1}{2}\right)\left(\frac{ckT}{N}\right)\tau_r \tag{21}$$

Here, it should be emphasized that this modification does not affect the use of the Brochard equations (3)−(5) for the Miesowicz viscosities, which remain unchanged. Equations 20 and 21 indicate that $\delta\alpha_2$ and $\delta\alpha_3$ are still dependent on the anisotropy ratio $R_\parallel/R_\perp$ but can now have different signs. Specifically, to obtain $\delta\alpha_2 > 0$ and $\delta\alpha_3 > 0$, eqs 20 and 21 require $R_\perp/R_\parallel > \sqrt{2}$. Combining eqs 20 and 21, we obtain

$$\delta\alpha_2/\delta\alpha_3 = \left(\frac{1}{2} - \frac{R_\parallel^2}{R_\perp^2}\right) \Big/ \left(\frac{R_\perp^2}{R_\parallel^2} - \frac{1}{2}\right) \tag{22}$$

which indicates that the ratio of the viscosity increments $\delta\alpha_2/\delta\alpha_3$ is solely a function of $R_\parallel/R_\perp$.

Equation 22 can be utilized to numerically compare the experimental values of $\delta\alpha_2/\delta\alpha_3$ at different nematic

Table 4. Leslie Viscosity Increments for 0.02 g/mL Side-Chain LCP (n = 5, DP = 71) in 5CB

temp (°C)	exptl result $\delta\alpha_2 \pm 20\%$ (Pa·s)	exptl result $\delta\alpha_3 \pm 5\%$ (Pa·s)	modified theory: $R_\parallel/R_\perp$ from ER $\delta\alpha_2 \pm 65\%$ (Pa·s)	modified theory: $R_\parallel/R_\perp$ from ER $\delta\alpha_3 \pm 100\%$ (Pa·s)	modified theory: $R_\parallel/R_\perp$ from stress transient $\delta\alpha_2 \pm 50\%$ (Pa·s)	modified theory: $R_\parallel/R_\perp$ from stress transient $\delta\alpha_3 \pm 100\%$ (Pa·s)
23	−0.0133	0.0088	−0.0114	0.0040	−0.0101	0.0056
25	−0.0141	0.0075	−0.0100	0.0035	−0.0099	0.0033
28	−0.0114	0.0063	−0.0097	0.0030	−0.0092	0.0042
31	−0.0146	0.0049	−0.0118	0.0019	−0.0116	0.0019

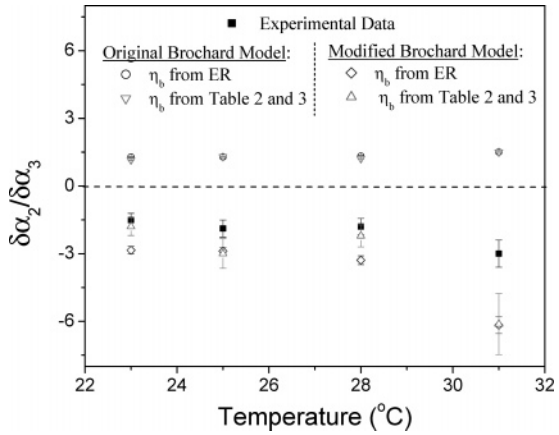

Figure 9. Temperature dependence of $\delta\alpha_2/\delta\alpha_3$ of a 0.02 g/mL solution of a side-chain LCP (n = 5, DP = 71) in 5CB.

temperatures with those calculated from the $R_\parallel/R_\perp$ values from $[\eta_{on}]/[\eta_{off}]$ data (Figure 4) via ER analysis and eq 8, or from $\delta\eta_e/\delta\eta_b$ data (Tables 2 and 3) and eq 5, using the original and modified Brochard theories. Such comparisons are shown in Figure 9 for an LCP concentration c = 0.02 g/mL. The modified theory clearly leads to improved semiquantitative agreement with experiment.

For completeness, in Table 4 experimental values for the viscosity increments $\delta\alpha_2$ and $\delta\alpha_3$ are compared vs values calculated from the revised theory (eqs 20 and 21) at c = 0.02 g/mL, using the two sets of $R_\parallel/R_\perp$ values referred to above, and prefactor $(kT\tau_r/N)$ from ER results.

Conclusions

The flow behavior of dilute solutions of a side-chain LCP (n = 5, DP = 71) in 5CB has been studied via ER and stress transient rheological measurements. The ratio of rms end-to-end distances $R_\parallel/R_\perp$ computed via the Brochard model, from values of $\delta\eta_b$ and $\delta\eta_e$ obtained by combining ER and stress transient analysis, were found to be numerically consistent with the ratio of global radii of gyration, $R_{g\parallel}/R_{g\perp}$, as well as the ratio of backbone radii, $R_{gb\parallel}/R_{gb\perp}$, obtained via SANS measurements, indicating that the SCLCP conformation is slightly prolate. Stress transient measurements show that dissolution of the side-chain LCP in 5CB (0.02 g/mL) alters the flow-aligning character of pure 5CB to a flow-tumbling behavior. This is strictly inconsistent with the Brochard theory, which predicts such a transition only for an oblate chain. Analysis of the stress transients at small strains via Ericksen's TIF theory yields values of the viscosity increments $\delta\alpha_2$ and $\delta\alpha_3$. Satisfactory agreement was obtained when comparing experimental values of $\delta\alpha_2$ and $\delta\alpha_3$ versus those calculated with $R_\parallel/R_\perp$ values derived from analysis of ER data, using a modified version of the Brochard theory, which incorporates an elastic coupling between the SCLCP and LMMN directors.

Acknowledgment. We gratefully acknowledge the financial support from the National Science Foundation Polymers Program through award DMR-0080114.

References and Notes

(1) Brochard, F. *J. Polym. Sci., Polym. Phys. Ed.* **1979**, *17*, 1367.
(2) Jamieson, A. M.; Gu, D.-F.; Chen, F.-L.; Smith, S. *Prog. Polym. Sci.* **1996**, *21*, 981.
(3) Casagrande, C.; Fabre, P.; Veyssie, M.; Weill, C.; Finkelmann, H. *Mol. Cryst. Liq. Cryst.* **1984**, *113*, 193.
(4) Mattoussi, H.; Veyssie, M. *J. Phys. (Paris)* **1989**, *50*, 99.
(5) Gu, D.-F.; Jamieson, A. M.; Rosenblatt, C.; Tomazos, D.; Lee, M.; Percec, V. *Macromolecules* **1991**, *24*, 2385.
(6) Weill, C.; Casagrande, C.; Veyssie, M. *J. Phys. II* **1986**, *47*, 887.
(7) Pashkovsky, E. E.; Litvina, T. G.; Kostromin, S.; Shibaev, V. P. *J. Phys. II* **1992**, *2*, 1577.
(8) Coles, H. J.; Sefton, M. S. *Mol. Cryst. Liq. Cryst. Lett.* **1985**, *1*, 159.
(9) Gu, D.-F.; Jamieson, A. M.; Lee, M.; Kawasumi, M.; Percec, V. *Liq. Cryst.* **1992**, *12*, 961.
(10) Gu, D.-F.; Jamieson, A. M.; Lee, M.; Kawasumi, M.; Percec, V. *Macromolecules* **1992**, *25*, 2151.
(11) Chen, F.-L.; Jamieson, A. M. *Macromolecules* **1994**, *27*, 1943.
(12) Chen, F.-L.; Jamieson, A. M.; Kawasumi, M.; Percec, V. *J. Polym. Sci., Polym. Phys.* **1995**, *33,* 1213.
(13) Gu, D.-F.; Jamieson, A. M.; Wang, S. Q. *J. Rheol.* **1993**, *37*, 985.
(14) Gu, D.-F.; Jamieson, A. M. *Macromolecules* **1994**, *27*, 337.
(15) Yao, N.; Jamieson, A. M. *Macromolecules* **1998**, *31*, 5399.
(16) Yao, N.; Jamieson, A. M. *J. Rheol.* **1998**, *42*, 603.
(17) Mattoussi, H.; Ober, R.; Veyssie, M.; Finkelmann, H. *Europhys. Lett.* **1986**, *2*, 233.
(18) Mattoussi, H.; Ober, R. *Macromolecules* **1990**, *23*, 1809.
(19) D'Allest, J. F.; Maïssa, A.; ten Bosch, A.; Sixou, P.; Blumstein, A.; Blumstein, R.; Teixeira, J.; Noirez, L. *Phys. Rev. Lett.* **1988**, *61*, 2562.
(20) D'Allest, J. F.; Sixou, P.; Blumstein, A.; Blumstein, R. B.; Teixeira, J.; Noirez, L. *Mol. Cryst. Liq. Cryst.* **1988**, *155*, 581.
(21) Kempe, M. D.; Kornfield, J. A. *Phys. Rev. Lett.* **2003**, *90*, 115501.
(22) Chiang, Y.-C.; Jamieson, A. M.; Campbell, S.; Lin, Y.; O'Sidocky, N. D.; Chien, L. C.; Kawasumi, M.; Percec, V. *Rheol. Acta* **1997**, *36*, 505.
(23) Chiang, Y.-C.; Jamieson, A. M.; Campbell, S.; Tong, T. H.; O'Sidocky, N. D.; Chien, L. C.; Kawasumi, M.; Percec, V. *Polymer* **2000**, *41*, 4127.
(24) Chiang, Y.-C.; Jamieson, A. M.; Kawasumi, M.; Percec, V. *Macromolecules* **1997**, *30*, 1992.
(25) Yao, N.; Jamieson, A. M. *Macromolecules* **1997**, *30*, 5822.
(26) Carri, G.; Muthukumar, M. *J. Chem. Phys.* **1998**, *109*, 11117.
(27) Cotton, J. P.; Hardouin, F. *Prog. Polym. Sci.* **1997**, *22*, 795.
(28) Chiang, Y.-C.; Jamieson, A. M.; Zhao, Y.; Kasko, A. M.; Pugh, C. *Polymer* **2002**, *43*, 4887.
(29) Yao, N.; Jamieson, A. M. *Rheol. Acta* **2000**, *39*, 338.
(30) Liu, P.-Y.; Yao, N.; Jamieson, A. M. *Macromolecules* **1999**, *32*, 6587.
(31) Liu, P.-Y.; Jamieson, A. M.; Yao, N. *Macromolecules* **2000**, *33*, 1692.
(32) Dong, S. S. Ph.D. Dissertation, Case Western Reserve University, Cleveland, 2004.
(33) Wu, S.-T.; Wang, Q.-H.; Kempe, M. D.; Kornfield, J. A. *J. Appl. Phys.* **2002**, *92*, 7146.
(34) Higgins, J. S.; Benoît, H. C. *Polymers and Neutron Scattering*; Clarendon Press: Oxford, 1994.
(35) Mather, P. T.; Pearson, D. S.; Larson, R. G.; Gu, D.; Jamieson, A. M. *Rheol. Acta* **1997**, *36*, 485.
(36) Zuniga, L.; Leslie, F. M. *Europhys. Lett.* **1989**, *9*, 689.
(37) Zuniga, L.; Leslie, F. M. *Liq. Cryst.* **1989**, *5*, 725.

(38) Burghardt, W. R. Ph.D. Thesis, Stanford University, Stanford, CA, 1990; Chapter 1.
(39) Han, H. W.; Rey, A. D. *J. Rheol.* **1995**, *39*, 301.
(40) Mather, P. T.; Pearson, D. S.; Larson, R. G. *Liq. Cryst.* **1996**, *20*, 527; *Liq. Cryst.* **1996**, *20*, 539.
(41) Gu. D.-F.; Jamieson, A. M. *J. Rheol.* **1994**, *38*, 555.
(42) Carlsson, T.; Skarp, K. *Mol. Cryst. Liq. Cryst.* **1981**, *78*, 157.
(43) Skarp, K.; Carsson, T.; Lagerwall, S. T.; Stebler, B. *Mol. Cryst. Liq. Cryst.* **1981**, *66*, 199.
(44) Kempe, M. D.; Kornfield, J. A.; Lal, J. *Macromolecules* **2004**, *37*, 8730.
(45) Guo, W.; Fung, B. M. *J. Chem. Phys.* **1991**, *95*, 3917.

MA050485H